

Article

β -Cyclodextrin-Modified Cotton Fabric for Medical and Hospital Applications with Photodynamic Antibacterial Activity Using Methylene Blue

Helen Beraldo Firmino¹, Emilly Karoline Tonini Silva Volante¹, Ana Claudia Pedrozo da Silva² ,
Fabio Alexandre Pereira Scacchetti² , Manuel José Lis^{3,*} , Meritxell Martí³ , Siddanth Saxena³ ,
André Luiz Tessaro^{1,2}  and Fabrício Maestá Bezerra^{1,*} 

¹ Post-Graduation Program in Materials Science and Engineering, Federal University of Technology, Apucarana 86812-460, Brazil; millyk.tonini@outlook.com (H.B.F.); emilly.karoline.tonini@gmail.com (E.K.T.S.V.); andretessaro@utfpr.edu.br (A.L.T.)

² Research Group of Active Materials, Federal University of Technology, Apucarana 86812-460, Brazil; anacsilva@utfpr.edu.br (A.C.P.d.S.); fabioscacchetti@utfpr.edu.br (F.A.P.S.)

³ Institute of Textile Research and Industrial, Cooperation of Terrassa, Universidad Politècnica de Catalunya (INTEXTER-UPC), 0822 Terrassa, Spain; meritxell.marti.gelabert@upc.edu (M.M.); siddanth.saxena@upc.edu (S.S.)

* Correspondence: manuel-jose.lis@upc.edu (M.J.L.); fabriciom@utfpr.edu.br (F.M.B.)

Abstract: The use of cyclodextrins in textiles for the development of biofunctional fabrics represents an interesting alternative for the advancement of dental, medical, and hospital materials. Cyclodextrins can interact with the chemical groups present in cotton fibers, leading to the formation of a nanostructured surface with specific functional properties, including antibacterial activity. Although there are numerous antibacterial textile finishes, the use of methylene blue as a cyclodextrin host molecule for photodynamic applications in textile materials remains to be investigated. This is because methylene blue is a photosensitive dye capable of generating singlet oxygen ($^1\text{O}_2$) when illuminated, which inactivates the pathogenic microorganisms that may be present in wounds. The objective of this study was to develop a biofunctionalized and photoactivatable cotton fabric with antimicrobial properties for use in the cosmetic or medical industries. The materials obtained were characterized via scanning electron microscopy (SEM), Fourier transform infrared spectroscopy with attenuated total reflection (FTIR-ATR), the determination of cotton fabric functionalization dyeing variables, colorimetry, UV-VIS spectrophotometry, degradation of 9,10-anthracenediyl-bis(methylene)dimalonic acid (ABDA), photodegradation tests, and microbiological analysis. The results showed that the textile was functionalized with β -cyclodextrin, mainly evidenced by the appearance of the band at 1730 cm^{-1} , indicating the formation of the ester group. Thus, when exposed to light, the non-functionalized material showed greater photobleaching, about 60%, compared to the material treated with cyclodextrin. This result was also reflected in the ABDA degradation kinetics, with the treated material showing 592.00% (first phase) and 966.20% (second phase) higher degradation than the untreated sample. Finally, the photodynamic activity was determined based on the antimicrobial properties of the textile, showing a reduction of more than 99% without exposure to light and 100% when exposed to light. It is believed that this study could open avenues for future research and the development of antimicrobial fabrics, as well as demonstrate the efficiency of the treatment with cyclodextrin in relation to photobleaching.

Keywords: photodynamic action; antimicrobial; biofunctional textile; cyclodextrin; methylene blue



Citation: Firmino, H.B.; Volante, E.K.T.S.; da Silva, A.C.P.; Scacchetti, F.A.P.; Lis, M.J.; Martí, M.; Saxena, S.; Tessaro, A.L.; Bezerra, F.M.

β -Cyclodextrin-Modified Cotton Fabric for Medical and Hospital Applications with Photodynamic Antibacterial Activity Using Methylene Blue. *Coatings* **2024**, *14*, 1100. <https://doi.org/10.3390/coatings14091100>

Academic Editors: Tsvetelina Batsalova and Denitsa Kiradzhiyska

Received: 10 July 2024

Revised: 21 August 2024

Accepted: 23 August 2024

Published: 1 September 2024



Copyright: © 2024 by the authors. Licensee MDPI, Basel, Switzerland. This article is an open access article distributed under the terms and conditions of the Creative Commons Attribution (CC BY) license (<https://creativecommons.org/licenses/by/4.0/>).

1. Introduction

Biofunctional textiles are gaining prominence due to their ability to absorb substances from the skin or release therapeutic or cosmetic compounds. Due to their interaction with

the skin, the use of textiles is a growing trend in technology, which helps combat diseases and provide additional benefits for the user [1–4]. Textiles with enhanced functionalities can find a variety of applications, such as the controlled release of active agents [5], cosmetotextiles [6], and temperature control [7]. Several techniques are employed to make textile materials biofunctional, such as microencapsulation [8], the use of mesoporous silica nanoparticles [9], metal-organic frameworks [10], and cyclodextrins [11].

The use of textiles as carriers for controlled-release devices and systems is characterized by their high skin contact area, drug-loading capacity, ease of application, low cost, stimulation release, biocompatibility, anti-allergic, and non-toxicity [12]. In this context, cyclodextrins (CDs) are becoming increasingly important due to their ability to encapsulate bioactive substances, their biocompatibility, and their acceptance in biological applications, allowing for the development of new finishes and the production of fabrics with new application possibilities [11,13–15]. Additionally, charged cyclodextrins are of significant interest for biomedical applications, as they offer protection to active molecules against detrimental external factors [16–18]. CDs are characterized as being oligosaccharides composed of glucose units organized in a truncated conical shape, which provides a well-defined cavity for the formation of a host–guest system and the ability to create these systems with a range of advantages [19,20]. Consisting of primary hydroxyl groups, the hydrogen atoms attached to the ether-type oxygen and polar hydrogen groups determine the hydrophobic character of the interior of the CD cavity, and the presence of free hydroxyl groups on the exterior gives these molecules a hydrophilic character.

In addition, with regard to the application of CDs in the textile industry, these, CDs can be used as leveling agents in dyeing [21,22] and in textile finishing [20,23–25], as well as for the complexation of drugs [14,19], dyes [11,13], essential oils, or phytoactives [26,27], cosmetics [28], and in biomedical applications [16,29]. The development of medical and hospital textiles is of significant interest, particularly concerning infectious diseases caused by pathogens [30]. Contact with contaminated surfaces can lead to serious illnesses and poses a significant problem for public health [31]. Therefore, the development of new finishes employing efficient techniques holds considerable value for both industry and society, Figure 1.



Figure 1. Application of a photodynamic dye on a textile substrate for the production of antimicrobial material for healthcare.

The inactivation of microorganisms is one of the functionalities being investigated in the field of biofunctional textiles. In this context, photodynamic inactivation (PDI) has emerged as a promising technique for controlling pathogenic microorganisms [32]. It is a branch of photodynamic therapy (PDT) and involves the application of a photosensitive compound (e.g., a dye) called a photosensitizer (PS) that preferentially accumulates in the cell membrane of the microorganisms [33]. Irradiation with appropriate light triggers a series of photophysical processes that can excite the PS to the triplet state ($^3\text{PS}^*$). Once the chromophore reaches $^3\text{PS}^*$, two mechanisms are proposed: in the type I mechanism, electrons are transferred between $^3\text{PS}^*$ and biological substrates, generating radical ions that subsequently react to form reactive oxygen species (ROS), such as the superoxide anion (O_2^-) and the hydroxyl radical (OH^\bullet). In the type II mechanism, energy is transferred from $^3\text{PS}^*$ directly to oxygen in its ground state leading to the formation of singlet oxygen ($^1\text{O}_2$), a highly oxidizing species. Both pathways result in cell death and can occur simultaneously, with the relative contributions of each mechanism depending on the photosensitizer used and the concentrations of substrate and/or oxygen present [34]. These species are responsible for nonspecific oxidative damage as they attack multiple molecular targets, such as lipids, proteins, and nucleic acids, promoting cell lysis and death [35]. In addition, PDI has not been shown to lead to bacterial resistance even after several cycles of partial killing and growth [34].

The photodynamic inactivation of microorganisms has been tested on Gram-positive and Gram-negative bacteria, such as *S. mutans*, *S. sanguis*, *S. aureus*, and *Lactobacillus* spp. with different types of photosensitizers, such as porphyrins, phenothiazines, and xanthenic dyes [36–39], which are present in the everyday human life. The bacterium *Staphylococcus aureus* is one of the most important human pathogens and develops complex mechanisms to evade the immune system, invade and efficiently damage host tissues, and cause various clinical syndromes, such as atopic dermatitis [40]. *S. aureus* has evolved to be resistant to almost all classes of antimicrobial agents, promoting the selection and spread of highly antibiotic-resistant strains. These strains can spread efficiently in community and hospital settings, dominating the *S. aureus* population structure and causing infections [41].

In this sense, phenothiazine dyes play a prominent role in PDI due to their remarkable photophysical properties, such as strong light absorption in the red-light region and an excellent ability to generate ROS. Methylene blue has long been used to detect premalignant cells and as a tissue marker in surgery. It has analgesic, antimicrobial, antitumor, and healing effects [42–45]. As a photosensitizer, it has advantages, such as low cost, easy application, and fewer side effects. MB can induce the formation of hydroxyl radicals (type I) or singlet oxygen species (type II), which further enhances its photodynamic effect [46–48]. The easy availability of MB and the ability to use polychromatic light sources make this dye a potential sensitizer for PDI that can be used in underserved populations for the treatment of a variety of diseases [49,50].

In this context, we investigate the functionalization of cotton fabric by incorporating β -cyclodextrin onto the textile surface through an esterification process, which results in a nanostructured surface with specific functional properties. Subsequently, the fabric is dyed with methylene blue, which acts as the guest molecule for the cyclodextrin. The outcome is an advanced and innovative cotton fabric capable of proactively combating infections through photodynamic therapy.

2. Materials and Methods

2.1. Materials

The materials β -CD (Cyclolab, Budapest, Hungary), citric acid (Synth, Diadema, Brazil), sodium hypophosphite monohydrate (Synth, Diadema, Brazil), sodium hydroxide (Synth, Diadema, Brazil), methylene blue (Dinâmica, Diadema, Brazil), and other analytical grade products were used without prior purification. The fabric used is 100% cotton (Brazil) with a weight of $228 \pm 5 \text{ g/m}^2$.

2.2. Methods

2.2.1. Cross-Linking of β -CD in Textiles

Initially, the amounts of β -CD, citric acid, and sodium hypophosphite monohydrate (SHP), the latter used as a catalyst for the reaction, were set at 100 g/L, 20 g/L, and 60 g/L, respectively.

The samples were immersed in a solution comprising 30 mL of distilled water for each gram of fabric (bath ratio 1:30). The described concentrations were used, and the samples were immersed in the solution for 10 min, following methodology adopted by Abdel-Halim and Al-Deyab [24] and Bezerra et al. [27].

Subsequently, the samples were subjected to the Pad-Dry-Cure process in a vertical foulard (Texcontrol, São Paulo, Brazil) with 100% pick-up, and then, they were dried at 110 °C for 3 min. The β -CD was crosslinked by curing in a Rama (Mathis, Oberhasli, Switzerland) for 3 min at a temperature of 190 °C. The entire experiment was performed in duplicate.

2.2.2. Methylene Blue Dyeing Method

Dyeing was carried out using an exhaustion process on a lab dyeing machine (Kimak AT1-SW, Brusque, Brazil). For the dyed samples, a fixed dye concentration of 6.25 μ M, a temperature of 50 °C, pH 10 (adjusted with NaOH), and a time of 1 h were used. UV-Vis spectrophotometry was employed to complement the factorial analysis of samples functionalized with and without β -CD and dyed with methylene blue. A UV-Vis absorption spectrophotometer (Cary 60, Agilent Technologies, Palo Alto, CA, USA) was utilized, with a spectral range of 190 to 1100 nm and a bandwidth of 1.5 nm. The samples were analyzed within the range of 200 to 800 nm, and the residual dye baths were also examined.

2.2.3. Statistical Treatment

The dyeing process is a multivariate process in which the amount of dye introduced into the fiber is dependent on several factors, including the temperature, initial concentrations, time, pH, and electrolyte content. Consequently, a study of the different parameters involved was conducted using ANOVA (software STUDIO R) with a 10% significance level. The values under consideration were treated at three levels: pH (4.0, 7.0 and 10.0), time (30, 45 and 60 min), temperature (50, 70, 90 °C), and NaCl concentration (0, 30 and 60 g/L). From these, the optimal conditions for the dyeing process were established using the residual dye concentration (RDC) and K/S as the response.

2.2.4. Characterization of the Materials

The following evaluation methods were used for the untreated 100% cotton fabric, the β -CD functionalized fabric, and the biofunctionalized fabric with dyes: Fourier transform attenuated total reflectance infrared spectroscopy (Thermo Fisher Scientific, Madison, WI, USA), scanning electron microscopy (JEOL Ltd., Tokyo, Japan), ultraviolet-visible light spectrophotometry (Agilent Technologies, Palo Alto, CA, USA), colorimetric analysis (PerkinElmer, Wellesley, MA, USA), microbiological analysis, singlet oxygen generation efficiency, and photodegradation of the textile materials.

Scanning Electron Microscopy

Samples of untreated 100% cotton fabric and β -CD-functionalized fabric were taken for electron microscopy analysis to assess the presence of β -CD on the fabric surface. The morphology of the cotton fabric was evaluated using a scanning electron microscope, JEOL-JSM 5610, coated with carbon.

Fourier Transform Attenuated Reflection Infrared Spectroscopy

FTIR-ATR was used to analyze the samples functionalized with β -CD, untreated 100% cotton fabrics, and the fabric functionalized with β -CD and washed after the esterification process. Scanning was performed at a wave number of 4000 to 500 cm^{-1} using the Nicolet

Avatar apparatus (Thermo Fisher Scientific, Madison, WI, USA), OMNIC software (version 6.2), and an ATR plate.

Photodegradation Test

To evaluate the photodegradation of MB in the paint samples, cold light was obtained by means of a fluorescent lamp used to simulate natural daylight, with a temperature of 6400 K and a luminous efficiency of 60 lm/W, information adapted from the technical standard BS-950-1. The light source used was positioned at a distance of 5.0 cm from the functionalized samples with and without β -CD and treated and dyed with AM, inside a closed booth. The samples were then measured with the colorimetric analysis (Spectrum 550 remission spectrophotometer, PerkinElmer, Wellesley, MA, USA), at time intervals of up to 72 h.

ABDA Degradation Kinetics

The singlet oxygen ($^1\text{O}_2$) generation was estimated via an indirect method using 9,10-anthracenediyl-bis(methylene)dimalonic acid (ABDA) as a probe. The reaction between $^1\text{O}_2$ and ABDA occurs through a cycloaddition (4 + 2) forming an endoperoxide (ABDA- O_2). Thus, the generation of singlet oxygen can be observed by the decrease in the ABDA absorption band at 400 nm [51,52].

All samples were monitored and illuminated using a set of warm white LEDs, with an emission range sufficient to excite the compound. The reactions were conducted in quartz cuvettes containing textile samples with and without β -CD and MB. In each experiment, the LED was positioned at a distance of 1.0 cm, resulting in an irradiance of 32 mW/cm² measured using an Ocean Optics Radiometer Spectrum model USB2000+ (Ocean Optics, Dunedin, FL, USA).

All the systems were kept under stirring conditions during the experiment. The solutions were prepared in distilled water. ABDA degradation kinetics were monitored in a UV-VIS (Varian Cary-60 spectrophotometer, Palo Alto, CA, USA) via scanning in kinetic mode.

Microbiological Analysis

The antibacterial activity of the functionalized fabrics was evaluated by adapting the AATCC 100—Test Method for Antibacterial Finishes on Textile Materials: Evaluation. The method was applied to the bacterium *Staphylococcus aureus* ATCC[®] 6538[™] (Gram-positive). To carry out the test, a new bacterial culture in sterile broth (TSB) was activated for 24 h at 37 ± 2 °C. The culture was then diluted in sterile buffer solution (PBS) to a concentration of approximately 1.5–3.0 × 10⁵ CFU/mL (0.5 McFarland). The samples were placed in a flask and inoculated with the suspension of microorganisms (500 µL volume).

The samples tested were divided into those exposed to a light source (white LED, 139.72 J/cm²) for 1 h and those kept in the dark for the same time. Immediately after the 1 h time, 50 mL of PBS was added to extract the bacteria, and the samples were serially diluted before being seeded on agar (in duplicate). As a positive control (textile sample without functionalization), the same concentration of CFU mL⁻¹ was serially diluted, and then, the standard plates were counted. The results were expressed as an average of the CFU mL⁻¹. The percentage reduction was determined according to Equation (1):

$$\text{Reduction \%} \left(\frac{\text{CFU}}{\text{mL}} \right) = \frac{B - A}{B} \times 100 \quad (1)$$

where A indicates the number of CFU mL⁻¹ for the bottle containing the finished textile sample after the contact time (illumination for 1 h), and B represents the number of CFU mL⁻¹ for the control sample. As a result, a colony count is carried out, and the values are averaged according to the agar plate counting method.

3. Results and Discussion

3.1. Analysis of the Fabric Treatment

Microscopy images of untreated and β -CD-treated cotton fabric are shown in Figure 2A,B, respectively. The images reveal twists in the cotton fibers caused by the spiraling of cellulose fibrils. The ribbon configuration with twists indicates a longitudinal view of the cotton. As illustrated in Figure 2B, the presence of β -CD can be observed on the surface of the treated cotton fabric, similar to the findings of Sundrarajan [53] and Alzate-Sánchez [54], attesting to the efficacy of the treatment.

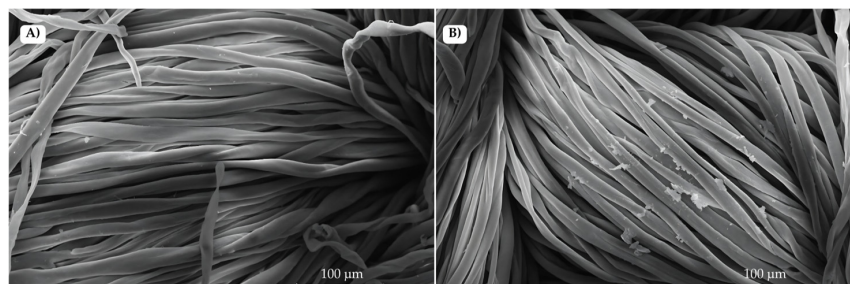


Figure 2. Scanning electron microscopy: (A) cotton and (B) cotton after treatment with β -CD.

The characterization of the material was also conducted via FTIR-ATR, as illustrated in Figure 3. The two curves shown demonstrate the presence of bands associated with the cellulose in the cotton fiber, including the following: at 3330 cm^{-1} , the O-H bond is responsible for the observed band, which is related to the β -glycosidic bridge (1-4). This is in addition to the band at 2930 cm^{-1} , which is due to stretching (C-H). Furthermore, the band at 1645 cm^{-1} is indicative of the C=C vibration in aromatic rings, while the C-O-C bond of the pyranose ring is observed at 1030 cm^{-1} . These bands are also evident in the works of Lis et al. [55]. Additionally, Figure 3B illustrates the emergence of a band in the 1730 cm^{-1} region, identified as an ester formed through the linkage of cotton with citric acid and the hydroxyl groups of β -CD. The band at 1730 cm^{-1} indicates the presence of cellulose carbonyl groups in three forms: esters, carboxylic acids, and carboxylate anions. An alkaline bath can convert the carboxylic group into a carboxylate anion, thereby highlighting the ester band [56,57]. Consequently, the sample treated with β -CD was washed with NaOH, and a new band at 1638 cm^{-1} was observed, confirming the existence of carboxylate anions. Nevertheless, the band at 1730 cm^{-1} persisted, thereby corroborating the ester bonds among β -CD, cotton, and citric acid. This result further substantiates the presence of β -CDs on the surface of the cotton fabric, consistent with the microscopic observations and suggesting that the finishing process was effective.

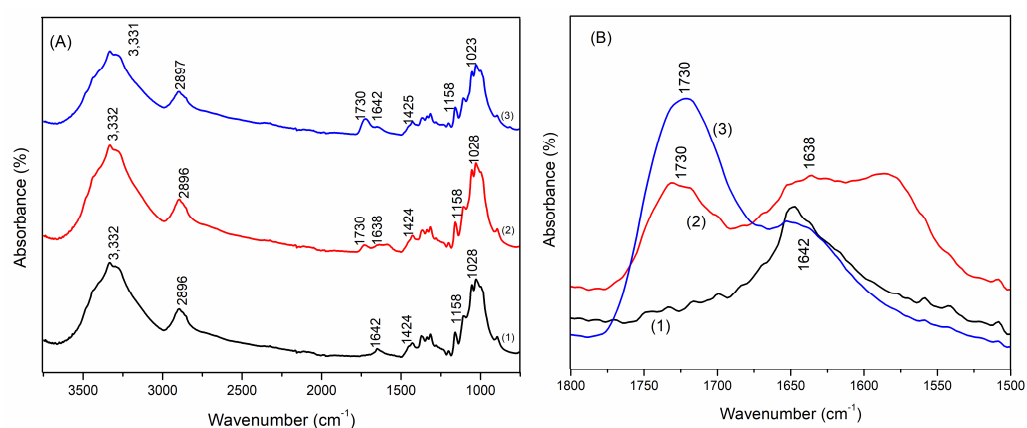


Figure 3. (A) ATR-FTIR spectrum and (B) its expansion in the region between 1800 and 1500 cm^{-1} of (1) cotton, (2) cotton with β -CD, and (3) cotton with β -CD after washing with NaOH.

3.2. Statistical Analysis of the Dyeing Process

In order to ascertain the optimal conditions for MB staining in cotton fabric, a series of variables was selected for investigation: pH, time, temperature, and NaCl concentration. These variables were observed to determine the extent to which they influence the residual dye concentration, with the objective of identifying the values that minimize or maximize this concentration. Additionally, the K/S parameter was chosen in response to the design matrix. Table 1 depicts the factorial design matrix, as well as the results obtained using the coloristic parameter (K/S) and residual dye concentration (RDC) as the response variables.

Table 1. Design matrix and experimental results considered in the factorial planning.

Sample	pH	Time (min)	Temperature (°C)	NaCl Concentration (g/L)	RDC (g/L)	K/S
1	4	30	50	0	0.001171	26.1172
2	10	30	50	0	0.000283	30.61208
3	4	60	50	0	0.001032	25.79435
4	10	60	50	0	0.00022	34.56379
5	4	30	90	0	0.001236	21.71599
6	10	30	90	0	0.000175	34.16909
7	4	60	90	0	0.000437	23.52474
8	10	60	90	0	0.000387	34.58468
9	4	30	50	60	0.000839	29.78177
10	10	30	50	60	0.000839	28.35535
11	4	60	50	60	0.000741	31.69385
12	10	60	50	60	0.000592	26.93975
13	4	30	90	60	0.001179	26.45997
14	10	30	90	60	0.001088	24.78423
15	4	60	90	60	0.001188	25.09617
16	10	60	90	60	0.001194	26.29626
17	7	45	70	30	0.001213	22.49068
18	7	45	70	30	0.001166	23.94341
19	7	45	70	30	0.001249	25.09617
20	7	60	70	30	0.001084	26.39438
21	7	30	70	30	0.001255	22.51928
22	7	45	70	30	0.001173	27.99113
23	7	45	50	30	0.00101	27.02324
24	7	45	70	0	0.000359	35.98995
25	7	45	70	30	0.001185	23.62882
26	10	45	70	30	0.001082	25.42733
27	7	45	70	60	0.000924	28.70613
28	7	45	90	30	0.001442	23.65863
29	7	45	70	30	0.001215	25.04917
30	4	45	70	30	0.00127	26.08476
31	7	45	70	30	0.00115	24.98661

Figure S1 presents the average values and the deviations of the considered variables in the experiment when RDC was used as the response variable. It can be seen that the absence of salt (NaCl = 0) produces the lowest levels of the residual dye concentration and, to confirm this fact, an analysis of variance was carried out considering only the factor NaCl concentration, which confirmed the hypothesis that an NaCl concentration equal to 0 g/L differs significantly from other NaCl concentrations. Therefore, only the results of NaCl = 0 were used for the following analyses.

The fitted model is shown in Equation (2), in which only the pH variable was significant at the 10% level (p -value = 0.03). It can be concluded that higher pH values lead to lower dye bath concentrations. The contour plots show that the lowest concentrations

(green in Figure S2) were achieved at the highest pH and time values and at the lowest temperatures, again highlighting that only pH was significant.

$$BC = 9.47 \times 10^{-4} - ph \times 1.79 \times 10^{-4} - time \times 6.60 \times 10^{-5} + temperature \times 8.88 \times 10^{-5} \quad (2)$$

To verify the effects of variables on K/S, the same preliminary procedure was adopted. Figure S3 shows that the highest K/S values are observed for a high pH and temperature and, apparently, for NaCl = 0. However, unlike what was observed in the study analyzing the residual concentration, the confidence intervals for the mean K/S for NaCl = 0 and NaCl = 60 overlap, indicating no significant difference.

Using ANOVA combined with variable selection methods, we found that the linear terms for the pH, time, temperature, and NaCl concentration were significant. Furthermore, the interactions among pH, temperature, and the NaCl concentration were significant, and the NaCl concentration was the only significant quadratic term that remained in the model. The final ANOVA model (Equation (3)) indicates that while the effects of time and the interaction between temperature and the NaCl concentration were not significant at the 10% level, their inclusion enhanced the model's performance, ensuring that there was no lack of fit. The time variable was the only one with a linear effect in the model, indicating that longer time durations resulted in higher K/S values.

$$\frac{K}{S} = 24.94 + ph \times 1.63 + time \times 0.57 - temperature \times 1.14 - NaCl \times 1.05 + pH : temperature \times 0.99 - pH : NaCl \times 2.71 - temperature : NaCl \times 0.69 + NaCl^2 \times 3.67 \quad (3)$$

Figure S4 shows the interaction fitted by the model presented in the Equation. Although it is not possible to determine a maximum point, we can conclude that the experimental conditions for achieving the maximum of KS is 60 min, 50 °C, pH 10, and the absence of NaCl. Those parameters are consistent with the interaction among MB, a cationic dye, and the OH groups of cotton, which are deprotonated at pH 10. Thus, the conditions were used in the dyeing process for both untreated and β -CD treated fabrics.

After the dyeing process, we investigated the release of MB from the fabrics. For this, a small sample of each fabric ($0.8 \times 0.8 \text{ cm}^2$) was put in contact with a PBS solution under constant stirring, and the UV-Vis spectra of the supernatant were collected over the time. The presence of β -CD subtly influences the release rate of MB in PBS but has a substantial impact on the percentage of dye released. For untreated fabrics, 9.5% of MB was released, whereas samples treated with β -CD released only 2% of the dye, resulting in nearly a five-fold reduction in the amount released. The impact of the β -CD on the dyeing process is also observed in the color intensity parameters and the photodegradation profile (see Section 3.4).

The residual baths from the MB depletion dyeing of fabrics, both with and without β -CD treatment, are shown in Figure 4. A superficial visual analysis reveals that the colors of the residual baths are lighter in the samples treated with β -CD. Theoretically, this suggests that the textile samples treated with β -CD will exhibit greater color intensity.



Figure 4. Residual baths from MB dyeing based on fabric untreated with β -CD (**left**) and MB dyeing based on fabric treated with β -CD (**right**).

Table 2 presents the initial and final concentrations of the dyeing process, allowing for the determination of the percentage of dye adsorbed by the fiber in each experiment.

Table 2. Residual dye bath with methylene blue dye on 100% cotton fabric treated and untreated with β -CD.

Sample	Initial Concentration (mg/L)	Final Concentration (mg/L)	Adsorption (%)
Untreated	25.60	3.50 ± 0.20	$86.14 \pm 0.94\%$
Treated with β -cyclodextrin	25.60	0.60 ± 0.17	$97.73 \pm 0.57\%$

Thus, it is observed that there is greater dye adsorption when the cotton fabric is treated with β -CD, at $97.73 \pm 0.57\%$. This is attributed to the increased interaction between the dye and the β -CD present on the fabric's surface, which, being rich in -OH groups, hosts the dyes more efficiently than untreated cotton.

3.3. Photobleaching Tests

It is well established that photosensitizers, such as methylene blue, undergo a photobleaching processes. Consequently, experiments were conducted to assess the impact of β -CD on this phenomenon, specifically examining the photobleaching process. Figure 5 illustrates the decline in color intensity (K/S) of the treated and untreated samples over 72 h, accompanied by images of the materials before (left) and after (right) exposure to light.

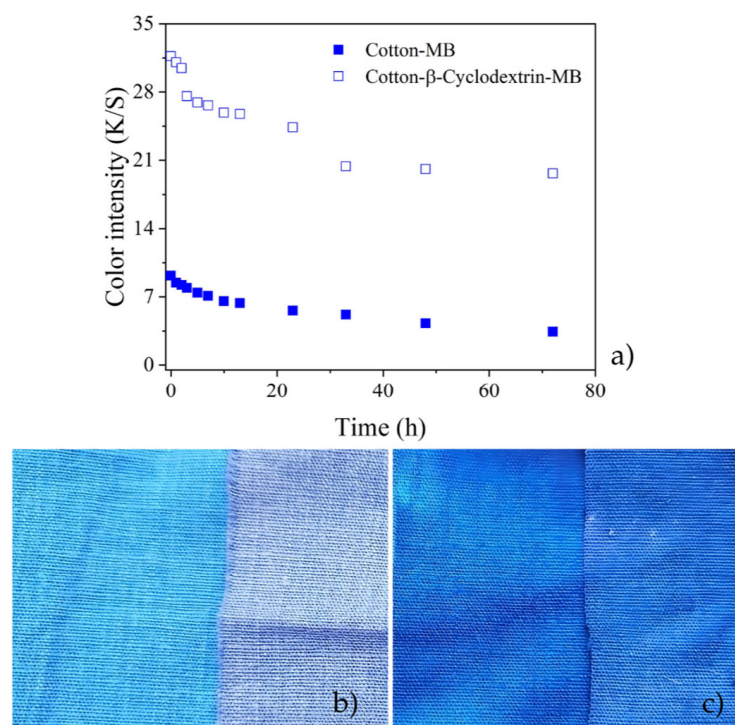


Figure 5. Photodegradation of MB dye, (a) Graph of light exposure (6400 K and a luminous efficiency of 60 lm/W) for cotton samples treated and untreated with cyclodextrin, cotton fabric samples: (b) untreated and (c) treated with β -CD.

The data indicate that the samples treated with β -CD and dyed with MB exhibit a higher color intensity compared to the sample that was not treated with β -CD and dyed with MB. In other words, samples that were not treated with β -CD exhibited a greater K/S loss following exposure to light, with a rate of approximately 60%. The graphs corroborate these results and demonstrate that the presence of β -CD in the samples reduces

the photobleaching rate of MB. This result is significant in the context of photodynamic action and material durability.

3.4. Kinetics of ABDA Degradation via Singlet Oxygen

To evaluate the formation of the singlet oxygen, the primary cytotoxic agent responsible for bacterial death, the well-established ABDA assay was performed. It has been demonstrated that fabric samples dyed in an aqueous medium can release singlet oxygen after illumination, which then reacts with the ABDA probe. Figure 6 depicts the decay of ABDA ($\lambda = 400 \text{ nm}$) as a function of the singlet oxygen release time. It is important to highlight that the experiments were also carried out in the dark as a control and that no reduction in the ABDA band was observed.

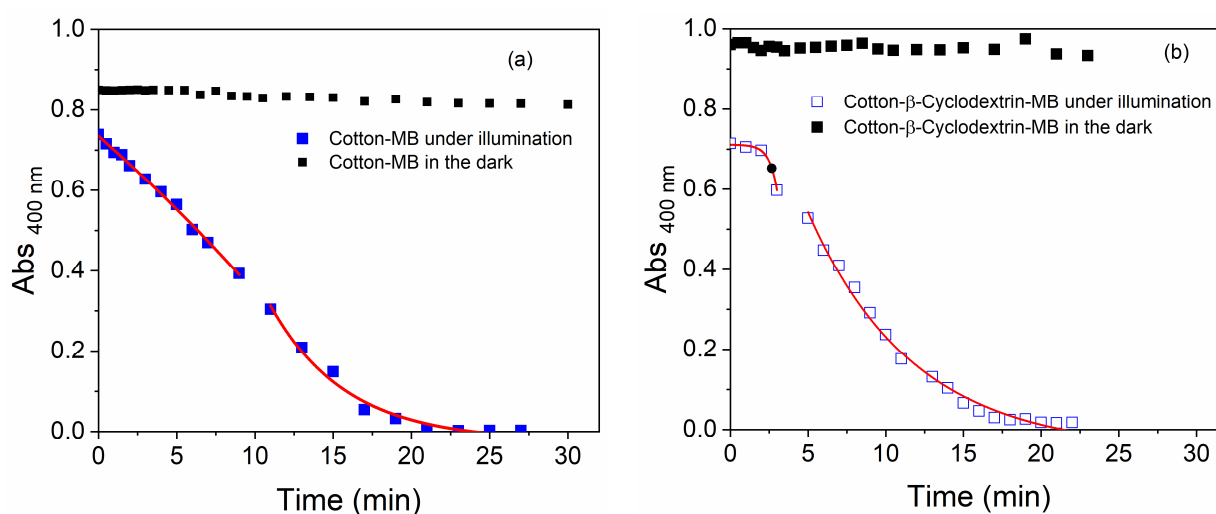


Figure 6. ABDA degradation rate of MB-dyed textile: (a) without treatment and (b) with β -CD. Black symbol: absorbance in the presence of light; red symbol: absorbance in the dark.

By adjusting Equation (4), it is possible to determine the ABDA decay rate and consequently the singlet oxygen formation rate in the presence of light.

$$y = y_0 \times e^{-\frac{k}{t}} \quad (4)$$

The adjustments showed that the fabric dyed with MB without β -CD exhibits two events with rates of 0.025 min^{-1} and 0.207 min^{-1} . The results indicate the presence of two distinct MB populations. It is conceivable that competition exists between two mechanisms: the diffusion of ABDA and its reaction with singlet oxygen ($^1\text{O}_2$), and the release of a small percentage of the dye into the aqueous medium. It is well established that the reaction of $^1\text{O}_2$ is highly dependent on its proximity to the target, given that its lifetime is extremely short. Consequently, it is probable that the degradation of ABDA (in the aqueous medium) from the $^1\text{O}_2$ generated by MB in the fibers will be slower. Nevertheless, the release of a percentage of this dye into the aqueous medium makes the Diels–Alder reaction considerably more favorable and, consequently, faster.

A similar result was observed for the material treated with β -CD. In this case, the events exhibited rate of 0.148 min^{-1} and 2.000 min^{-1} , respectively. For an easier comparison, the data are listed in Table 3.

Table 3. ABDA degradation kinetics of fabric dyed with MB.

Material	Kinetic Rate (First Phase)	Kinetic Rate (Second Phase)
Untreated	0.025 min ⁻¹	0.207 min ⁻¹
Treated with β -cyclodextrin ratio	0.148 min ⁻¹ 592.00%	2.000 min ⁻¹ 966.20%

It was observed that the presence of β -CD resulted in an acceleration of the reaction between ¹O₂ and ABDA. This phenomenon can be elucidated by considering the results of the photobleaching tests. As illustrated in Figure 5, the materials treated with cyclodextrin exhibited a more intense color even in the absence of illumination. It can be posited that the presence of this binder enhanced the interaction between the fabric and the MB, thereby facilitating dyeing. Moreover, β -CD protected the dye from photobleaching processes, thereby enhancing its photodynamic action. Consequently, the generation of singlet oxygen is likely to be greater in the treated sample, as, in addition to having more MB molecules, these are not degraded as easily.

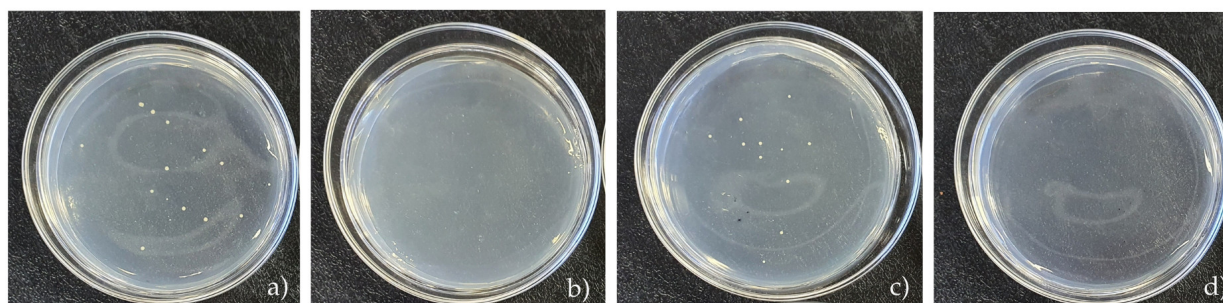
3.5. Microbiological Analysis

The microbiological analysis tests are conducted to verify the effectiveness of the textile finish and validate the antibacterial properties of the cotton fabric. This validation is crucial as the fabric is intended for use as a biofunctional textile to prevent bacterial proliferation on the skin. Table 4 presents the observed reduction in the bacterial count.

Table 4. Antibacterial reduction, using *S. aureus* bacteria and a control containing 2.6×10^5 CFU mL⁻¹, in fabrics untreated and treated with β -cyclodextrin under the same conditions.

Samples	N. of Bacteria (CFU mL ⁻¹) in 1 h	Reduction (%)
MB (no light)	1.5×10^3	99.42
MB	0	100
MB + β -CD (no light)	1.1×10^3	99.57
MB + β -CD	0	100

From the data presented in Table 4 and Figure 7, it can be observed that there was a significant degree of bacterial inactivation even in the absence of light. This property of MB has already been described in the literature and can be observed at high concentrations [58]. Nevertheless, it is also evident that the system exhibits a photodynamic effect, with complete bacterial inactivation achieved following illumination.

**Figure 7.** Microbiological analysis of samples: (a) dyed fabric with MB, not treated with β -CD, in the absence of light; (b) dyed fabric with MB, not treated with β -CD, in the presence of light; (c) dyed fabric with MB, treated with β -CD, in the absence of light; (d) dyed fabric with MB, treated with β -CD, in the presence of light.

Miazaki et al. [59] and colleagues also tested the *S. aureus* bacterium in their work on photodynamic inactivation with MB and obtained results that confirmed its beneficial antibacterial properties against Gram-positive organisms. The *S. aureus* bacterium is currently a significant concern in human skin health. The development of cosmetotextiles and dressings that prevent the proliferation of this bacterium is a topic of interest in the medical and hospital environments [60]. It is evident that MB exhibits exceptional microbial inactivation capabilities, achieving rates above 99.42% for MB samples. This makes it an ideal choice for use as a photosensitizer in antimicrobial skin treatments [61].

4. Conclusions

The use of cyclodextrins in textiles for the development of biofunctional fabrics represents an alternative approach for creating medical materials. The integration of cyclodextrin molecules at the nanoscale onto the surface of cotton fibers created a nanostructured surface with functional properties. Cyclodextrins can be used to complex with active molecules that will be released, such as dyes and drugs. The study indicates that the MB dye exhibits a significant reduction in bacterial viability, particularly in the presence of light, due to the generation of singlet oxygen. Even in the absence of direct light exposure, the presence of MB results in antimicrobial effects. MB appears to be a promising candidate for use as a photosensitizer in cutaneous antimicrobial treatments.

Finally, in addition to all the aforementioned advantages of using β -CD to dye cotton fibers, in the specific case of developing materials with photodynamic potential, the presence of cyclodextrin plays an additional role in protecting the dyes from photodegradation, allowing the useful life of the material to be longer than that of samples not treated with β -CD, without altering its antimicrobial capacity.

Supplementary Materials: The following supporting information can be downloaded at: <https://www.mdpi.com/article/10.3390/coatings14091100/s1>, Figure S1: Means and standard deviations of residual dye concentration based on each level of variables in the study: (a) pH, (b) time (min.), (c) temperature, and (d) NaCl concentration.; Figure S2: Contour plots for the fitted model (a) split at 70 °C, (b) split at 45 min, and (c) split at pH 7; Figure S3: Means and standard deviations of K/S based on each level of variables in the study: (a) pH, (b) time (min.), (c) temperature, and (d) NaCl concentration; Figure S4: Fitted effects on K/S of interactions in the model for samples dyed with MB, (a) fixed at an NaCl concentration [45 g/L], (b) fixed at a temperature of 70 °C, and (c) fixed at pH 7.

Author Contributions: Conceptualization, A.L.T. and F.M.B.; methodology, A.C.P.d.S., M.J.L. and A.L.T.; formal analysis, H.B.F.; investigation, H.B.F. and E.K.T.S.V.; data curation, H.B.F., A.C.P.d.S., F.A.P.S., A.L.T., M.M., S.S. and F.M.B.; writing—original draft preparation, H.B.F., S.S. and E.K.T.S.V.; writing—review and editing, M.J.L., M.M., S.S. and F.M.B.; visualization, F.M.B. and M.M.; supervision, A.L.T.; project administration, M.J.L.; funding acquisition, M.J.L. and F.M.B. All authors have read and agreed to the published version of the manuscript.

Funding: This research was funded by CNPq—Conselho Nacional de Desenvolvimento Científico e Tecnológico, process number 420280/2023-5 (A.L.T.) and 201166/2024-0 (F.M.B).

Institutional Review Board Statement: Not applicable.

Informed Consent Statement: Not applicable.

Data Availability Statement: Data are contained within the article and Supplementary Materials.

Acknowledgments: CNPq—Conselho Nacional de Desenvolvimento Científico e Tecnológico, of the Ministry of Science, Technology and Innovation, UPC and the Laboratório Multiusuário (LAMAP) at UTFPR—Apucarana campus.

Conflicts of Interest: The authors declare no conflicts of interest.

References

1. Ma, J.; Fan, J.; Xia, Y.; Kou, X.; Ke, Q.; Zhao, Y. Preparation of Aromatic β -Cyclodextrin Nano/Microcapsules and Corresponding Aromatic Textiles: A Review. *Carbohydr. Polym.* **2023**, *308*, 120661. [[CrossRef](#)] [[PubMed](#)]
2. Shah, M.A.; Pirzada, B.M.; Price, G.; Shibiru, A.L.; Qurashi, A. Applications of Nanotechnology in Smart Textile Industry: A Critical Review. *J. Adv. Res.* **2022**, *38*, 55–75. [[CrossRef](#)]
3. Mendes, S.; Catarino, A.; Zille, A.; Fernandes, N.; Bezerra, F.M. Vehiculation of Methyl Salicylate from Microcapsules Supported on Textile Matrix. *Materials* **2021**, *14*, 1087. [[CrossRef](#)] [[PubMed](#)]
4. Ma, L.L.; Wei, Y.-Y.; Li, J.; Sun, Y.-Y.; Liu, S.R.; Ma, K.M.; Leung, P.H.-M.; Tao, X.M. Clinical Study of Antibacterial Medical Textiles Containing Polyhydroxyalkanoate Oligomers for Reduction of Hospital-Acquired Infections. *J. Hosp. Infect.* **2024**, *149*, 144–154. [[CrossRef](#)]
5. Valle, J.A.B.; Curto Valle, R.D.C.S.; Da Costa, C.; Maestá, F.B.; Lis Arias, M.J. Reservoir Effect of Textile Substrates on the Delivery of Essential Oils Microencapsulated by Complex Coacervation. *Polymers* **2024**, *16*, 670. [[CrossRef](#)] [[PubMed](#)]
6. Azizi, N.; Chevalier, Y.; Majdoub, M. Isosorbide-Based Microcapsules for Cosmeto-Textiles. *Ind. Crops Prod.* **2014**, *52*, 150–157. [[CrossRef](#)]
7. Emam, H.E.; Abdelhameed, R.M. In-Situ Modification of Natural Fabrics by Cu-BTC MOF for Effective Release of Insect Repellent (N,N-Diethyl-3-Methylbenzamide). *J. Porous Mater.* **2017**, *24*, 1175–1185. [[CrossRef](#)]
8. Jiao, M.; Zhang, Y.; Dong, Z.; Zhang, H.; Jiang, Y. Microencapsulation of Multi-Component Traditional Chinese Herbs Extracts and Its Application to Traditional Chinese Medicines Loaded Textiles. *Colloids Surf. B Biointerfaces* **2024**, *240*, 113970. [[CrossRef](#)]
9. Da Silva, A.C.P.; Arruda, L.M.; Moreira, I.P.; Scacchetti, F.A.P.; De Oliveira, H.P.M.; Samulewski, R.B.; Figueiro, R.; Tessaro, A.L. Functionalization of Fibrous Substrates with Mesoporous Silica Nanoparticles as a Strategy to Obtain Photodynamic Antibacterial Textiles. *Dye. Pigment.* **2024**, *230*, 112342. [[CrossRef](#)]
10. Rahman, M.; Kabir, M.; Chen, S.; Wu, S. Developments, Applications, and Challenges of Metal–Organic Frameworks@textile Composites: A State-of-Art Review. *Eur. Polym. J.* **2023**, *199*, 112480. [[CrossRef](#)]
11. Bezerra, F.M.; Lis, M.J.; Firmino, H.B.; Dias Da Silva, J.G.; Curto Valle, R.D.C.S.; Borges Valle, J.A.; Scacchetti, F.A.P.; Tessaro, A.L. The Role of β -Cyclodextrin in the Textile Industry—Review. *Molecules* **2020**, *25*, 3624. [[CrossRef](#)] [[PubMed](#)]
12. Sun, X.-Z.; Wang, X.; Wu, J.-Z.; Li, S.-D. Development of Thermosensitive Microgel-Loaded Cotton Fabric for Controlled Drug Release. *Appl. Surf. Sci.* **2017**, *403*, 509–518. [[CrossRef](#)]
13. Crini, G. Review: A History of Cyclodextrins. *Chem. Rev.* **2014**, *114*, 10940–10975. [[CrossRef](#)]
14. Nardello-Rataj, V.; Leclercq, L. Encapsulation of Biocides by Cyclodextrins: Toward Synergistic Effects against Pathogens. *Beilstein J. Org. Chem.* **2014**, *10*, 2603–2622. [[CrossRef](#)]
15. Fernández, M.A.; Silva, O.F.; Vico, R.V.; De Rossi, R.H. Complex Systems That Incorporate Cyclodextrins to Get Materials for Some Specific Applications. *Carbohydr. Res.* **2019**, *480*, 12–34. [[CrossRef](#)]
16. Sehgal, V.; Pandey, S.P.; Singh, P.K. Prospects of Charged Cyclodextrins in Biomedical Applications. *Carbohydr. Polym.* **2024**, *323*, 121348. [[CrossRef](#)] [[PubMed](#)]
17. Alishahi, M.; Aboelkheir, M.; Chowdhury, R.; Altier, C.; Shen, H.; Uyar, T. Functionalization of Cotton Nonwoven with Cyclodextrin/Lawsone Inclusion Complex Nanofibrous Coating for Antibacterial Wound Dressing. *Int. J. Pharm.* **2024**, *652*, 123815. [[CrossRef](#)] [[PubMed](#)]
18. Garg, A.; Alfatease, A.; Hani, U.; Haider, N.; Akbar, M.J.; Talath, S.; Angolkar, M.; Paramshetti, S.; Osmani, R.A.M.; Gundawar, R. Drug Eluting Protein and Polysaccharides-Based Biofunctionalized Fabric Textiles- Pioneering a New Frontier in Tissue Engineering: An Extensive Review. *Int. J. Biol. Macromol.* **2024**, *268*, 131605. [[CrossRef](#)]
19. Rasheed, A. Cyclodextrins as Drug Carrier Molecule: A Review. *Sci. Pharm.* **2008**, *76*, 567–598. [[CrossRef](#)]
20. Nostro, P.L.; Fratoni, L.; Ridi, F.; Baglioni, P. Surface Treatments on Tencel Fabric: Grafting with β -cyclodextrin. *J. Appl. Polym. Sci.* **2003**, *88*, 706–715. [[CrossRef](#)]
21. Bezerra, F.M.; Carvalho Cotre, D.S.D.; Plath, A.; Firmino, H.B.; Lima, M.A.D.; Lis, M.; Samulewski, R.B.; Moisés, M.P. β -Cyclodextrin: Disperse Yellow 211 Complexes Improve Coloristic Intensity of Polyamide Dyed Knits. *Text. Res. J.* **2022**, *92*, 2194–2204. [[CrossRef](#)]
22. Ferreira, B.T.M.; Espinoza-Quñones, F.R.; Borba, C.E.; Módenes, A.N.; Santos, W.L.F.; Bezerra, F.M. Use of the β -Cyclodextrin Additive as a Good Alternative for the Substitution of Environmentally Harmful Additives in Industrial Dyeing Processes. *Fibers Polym.* **2020**, *21*, 1266–1274. [[CrossRef](#)]
23. Crupi, V.; Ficarra, R.; Guardo, M.; Majolino, D.; Stancanelli, R.; Venuti, V. UV–Vis and FTIR–ATR Spectroscopic Techniques to Study the Inclusion Complexes of Genistein with β -Cyclodextrins. *J. Pharm. Biomed. Anal.* **2007**, *44*, 110–117. [[CrossRef](#)]
24. Abdel-Halim, E.S.; Al-Deyab, S.S.; Alfaifi, A.Y.A. Cotton Fabric Finished with β -Cyclodextrin: Inclusion Ability toward Antimicrobial Agent. *Carbohydr. Polym.* **2014**, *102*, 550–556. [[CrossRef](#)]
25. Marques, H.M.C. A Review on Cyclodextrin Encapsulation of Essential Oils and Volatiles. *Flavour. Fragr. J.* **2010**, *25*, 313–326. [[CrossRef](#)]
26. Pinho, E.; Grootveld, M.; Soares, G.; Henriques, M. Cyclodextrins as Encapsulation Agents for Plant Bioactive Compounds. *Carbohydr. Polym.* **2014**, *101*, 121–135. [[CrossRef](#)] [[PubMed](#)]
27. Maestá Bezerra, F.; García Carmona, Ó.; García Carmona, C.; Souza Plath, A.M.; Lis, M. Biofunctional Wool Using β -Cyclodextrins as Vehiculizer of Citronella Oil. *Process Biochem.* **2019**, *77*, 151–158. [[CrossRef](#)]

28. Radu, C.-D.; Parteni, O.; Ochiuz, L. Applications of Cyclodextrins in Medical Textiles—Review. *J. Control. Release* **2016**, *224*, 146–157. [[CrossRef](#)]
29. Huang, T.; Hu, X.; Huang, S.; Liu, D.; Chen, L.; Wu, Q.; Zhu, W.; Zhang, X.; Liu, M.; Wei, Y. One-Step Synthesis of Cyclodextrin-Based Fluorescent Hyperbranched Polymer as Type I Photosensitizer for Effective Photodynamic Therapy. *Dye. Pigment.* **2024**, *223*, 111928. [[CrossRef](#)]
30. Zhang, N.; Xu, Y.; Shi, R.; Zhou, M.; Yu, Y.; Wang, P.; Wang, Q. Protein-Based Coating Strategy for Preparing Durable Sunlight-Driven Rechargeable Antibacterial, Super Hydrophilic, and UV-Resistant Textiles. *Int. J. Biol. Macromol.* **2024**, *258*, 128761. [[CrossRef](#)]
31. Li, J.; Wang, X.; Wang, H.; Ran, P.; Liu, Y.; Wang, J.; Xu, X.; Zhou, Z. Regulating Molecular Brush Structure on Cotton Textiles for Efficient Antibacterial Properties. *Int. J. Biol. Macromol.* **2024**, *267*, 131486. [[CrossRef](#)]
32. Mali, S.B.; Dahivelkar, S.D.; Mahale, S.A. Nanotechnology in Photodynamic Therapy. *Oral. Oncol. Rep.* **2024**, *10*, 100307. [[CrossRef](#)]
33. Lu, B.; Lu, X.; Mu, M.; Meng, S.; Feng, Y.; Zhang, Y. Novel Near-Infrared BODIPY-Cyclodextrin Complexes for Photodynamic Therapy. *Heliyon* **2024**, *10*, e26907. [[CrossRef](#)] [[PubMed](#)]
34. Hamblin, M.R. Antimicrobial Photodynamic Inactivation: A Bright New Technique to Kill Resistant Microbes. *Curr. Opin. Microbiol.* **2016**, *33*, 67–73. [[CrossRef](#)]
35. Cieplik, F.; Deng, D.; Crielaard, W.; Buchalla, W.; Hellwig, E.; Al-Ahmad, A.; Maisch, T. Antimicrobial Photodynamic Therapy—What We Know and What We Don't. *Crit. Rev. Microbiol.* **2018**, *44*, 571–589. [[CrossRef](#)]
36. Zeyada, H.M.; El-Mallah, H.M.; Atwee, T.; El-Damhogi, D.G. Spectroscopic Studies of UV Irradiated Erythrosine B Thin Films Prepared by Spin Coating Technique. *Spectrochim. Acta Part A Mol. Biomol. Spectrosc.* **2017**, *179*, 120–124. [[CrossRef](#)] [[PubMed](#)]
37. Kim, J.R.; Michielsen, S. Photodynamic Activity of Nanostructured Fabrics Grafted with Xanthene and Thiazine Dyes against Opportunistic Fungi. *J. Photochem. Photobiol. B Biol.* **2015**, *150*, 50–59. [[CrossRef](#)] [[PubMed](#)]
38. Silva, A.F.; Borges, A.; Freitas, C.F.; Hioka, N.; Mikcha, J.M.G.; Simões, M. Antimicrobial Photodynamic Inactivation Mediated by Rose Bengal and Erythrosine Is Effective in the Control of Food-Related Bacteria in Planktonic and Biofilm States. *Molecules* **2018**, *23*, 2288. [[CrossRef](#)]
39. Slyusareva, E.; Szykh, A.; Tyagi, A.; Penzkofer, A. Spectral and Photophysical Properties of Fluorone Dyes in Bio-Related Films and Methanol. *J. Photochem. Photobiol. A Chem.* **2009**, *208*, 131–140. [[CrossRef](#)]
40. Leyva-Castillo, J.-M.; McGurk, A.; Geha, M.D.R. Allergic Skin Inflammation and *S. Aureus* Skin Colonization Are Mutually Reinforcing. *Clin. Immunol.* **2020**, *218*, 108511. [[CrossRef](#)]
41. Lima, W.G.; De Brito, J.C.M.; Cardoso, V.N.; Fernandes, S.O.A. In-Depth Characterization of Antibacterial Activity of Melittin against *Staphylococcus Aureus* and Use in a Model of Non-Surgical MRSA-Infected Skin Wounds. *Eur. J. Pharm. Sci.* **2021**, *156*, 105592. [[CrossRef](#)] [[PubMed](#)]
42. Krishnaswami, V.; Natarajan, B.; Sethuraman, V.; Natesan, S.; RajSelvaraj, B. Nano Based Photodynamic Therapy to Target Tumor Microenvironment. *Nano Trends* **2023**, *1*, 100003. [[CrossRef](#)]
43. Dey, A.; Singhvi, G.; Puri, A.; Kesharwani, P.; Dubey, S.K. An Insight into Photodynamic Therapy towards Treating Major Dermatological Conditions. *J. Drug Deliv. Sci. Technol.* **2022**, *76*, 103751. [[CrossRef](#)] [[PubMed](#)]
44. Pérez, C.; Zúñiga, T.; Palavecino, C.E. Photodynamic Therapy for Treatment of *Staphylococcus Aureus* Infections. *Photodiagn. Photodyn. Ther.* **2021**, *34*, 102285. [[CrossRef](#)] [[PubMed](#)]
45. Sadraian, M.; Zhang, L.; Aavani, F.; Biazar, E.; Jin, D. Photodynamic Viral Inactivation Assisted by Photosensitizers. *Mater. Today Phys.* **2022**, *28*, 100882. [[CrossRef](#)]
46. Jiang, J.; Lv, X.; Cheng, H.; Yang, D.; Xu, W.; Hu, Y.; Song, Y.; Zeng, G. Type I Photodynamic Antimicrobial Therapy: Principles, Progress, and Future Perspectives. *Acta Biomater.* **2024**, *177*, 1–19. [[CrossRef](#)]
47. Boltos Cecatto, R.; Siqueira De Magalhães, L.; Fernanda Setúbal Destro Rodrigues, M.; Pavani, C.; Lino-dos-Santos-Franco, A.; Teixeira Gomes, M.; Fátima Teixeira Silva, D. Methylene Blue Mediated Antimicrobial Photodynamic Therapy in Clinical Human Studies: The State of the Art. *Photodiagn. Photodyn. Ther.* **2020**, *31*, 101828. [[CrossRef](#)]
48. Alasqah, M.N. Efficacy of Methylene Blue-Mediated Antimicrobial Photodynamic Therapy on Clinical and Radiographic Outcomes among Patients with Periodontal Diseases: A Systematic Review and Meta-Analysis of Randomized Controlled Trials. *Photodiagn. Photodyn. Ther.* **2024**, *46*, 104000. [[CrossRef](#)]
49. Tardivo, J.P.; Del Giglio, A.; De Oliveira, C.S.; Gabrielli, D.S.; Junqueira, H.C.; Tada, D.B.; Severino, D.; De Fátima Turchiello, R.; Baptista, M.S. Methylene Blue in Photodynamic Therapy: From Basic Mechanisms to Clinical Applications. *Photodiagn. Photodyn. Ther.* **2005**, *2*, 175–191. [[CrossRef](#)]
50. Garapati, C.; Boddu, S.H.; Jacob, S.; Ranch, K.M.; Patel, C.; Babu, R.J.; Tiwari, A.K.; Yasin, H. Photodynamic Therapy: A Special Emphasis on Nanocarrier-Mediated Delivery of Photosensitizers in Antimicrobial Therapy. *Arab. J. Chem.* **2023**, *16*, 104583. [[CrossRef](#)]
51. Bergmann, E.V.; Capeloto, O.A.; Catanio, A.T.S.; Flizikowski, G.A.S.; Kimura, N.M.; Freitas, C.F.; Herculano, L.S.; Astrath, N.G.C.; Malacarne, L.C. Photoactivation of Erythrosine in Simulated Body Fluids. *Spectrochim. Acta Part A Mol. Biomol. Spectrosc.* **2021**, *259*, 119867. [[CrossRef](#)] [[PubMed](#)]
52. Entradas, T.; Waldron, S.; Volk, M. The Detection Sensitivity of Commonly Used Singlet Oxygen Probes in Aqueous Environments. *J. Photochem. Photobiol. B Biol.* **2020**, *204*, 111787. [[CrossRef](#)] [[PubMed](#)]

53. Rukmani, A.; Sundrarajan, M. Inclusion of Antibacterial Agent Thymol on β -Cyclodextrin-Grafted Organic Cotton. *J. Ind. Text.* **2012**, *42*, 132–144. [[CrossRef](#)]
54. Alzate-Sánchez, D.M.; Smith, B.J.; Alsaiee, A.; Hinestroza, J.P.; Dichtel, W.R. Cotton Fabric Functionalized with a β -Cyclodextrin Polymer Captures Organic Pollutants from Contaminated Air and Water. *Chem. Mater.* **2016**, *28*, 8340–8346. [[CrossRef](#)]
55. Lis, M.J.; García Carmona, Ó.; García Carmona, C.; Maestá Bezerra, F. Inclusion Complexes of Citronella Oil with β -Cyclodextrin for Controlled Release in Biofunctional Textiles. *Polymers* **2018**, *10*, 1324. [[CrossRef](#)]
56. Medronho, B.; JM Valente, A.; Costa, P.; Romano, A. Inclusion Complexes of Rosmarinic Acid and Cyclodextrins: Stoichiometry, Association Constants, and Antioxidant Potential. *Colloid. Polym. Sci.* **2014**, *292*, 885–894. [[CrossRef](#)]
57. Voncina, B.; Le Marechal, A.M. Grafting of Cotton with B-cyclodextrin via Poly(Carboxylic Acid). *J. Appl. Polym. Sci.* **2005**, *96*, 1323–1328. [[CrossRef](#)]
58. Wainwright, M. Tricyclic Cationic Chromophores as Models for New Photoantimicrobials. *J. Braz. Chem. Soc.* **2015**, *26*, 2390–2404. [[CrossRef](#)]
59. Miazaki, J.B.; Dos Santos, A.R.; De Freitas, C.F.; Stafussa, A.P.; Mikcha, J.M.G.; Bergamasco, R.D.C.; Tonon, L.A.C.; Madrona, G.S.; Caetano, W.; Da Silva, L.H.; et al. Edible Coatings and Application of Photodynamics in Ricotta Cheese Preservation. *LWT* **2022**, *165*, 113697. [[CrossRef](#)]
60. Hakimov, S.; Kylychbekov, S.; Harness, B.; Neupane, S.; Hurley, J.; Brooks, A.; Banga, S.; Er, A.O. Evaluation of Silver Nanoparticles Attached to Methylene Blue as an Antimicrobial Agent and Its Cytotoxicity. *Photodiagn. Photodyn. Ther.* **2022**, *39*, 102904. [[CrossRef](#)]
61. Feng, Y.; Tonon, C.C.; Hasan, T. Dramatic Destruction of Methicillin-Resistant Staphylococcus Aureus Infections with a Simple Combination of Amoxicillin and Light-Activated Methylene Blue. *J. Photochem. Photobiol. B Biol.* **2022**, *235*, 112563. [[CrossRef](#)] [[PubMed](#)]

Disclaimer/Publisher’s Note: The statements, opinions and data contained in all publications are solely those of the individual author(s) and contributor(s) and not of MDPI and/or the editor(s). MDPI and/or the editor(s) disclaim responsibility for any injury to people or property resulting from any ideas, methods, instructions or products referred to in the content.